

Phonon Scattering in Sodium Chloride Containing Oxygen*

MILES V. KLEINT†

Laboratory of Atomic and Solid-State Physics, Cornell University, Ithaca, New York

(Received January 30, 1961)

The thermal conductivity of supposedly pure NaCl crystals from several sources was found to vary by as much as two orders of magnitude at low temperatures. The conductivity of Harshaw crystals was particularly low. This effect was quantitatively related to the presence of an ultraviolet absorption band at 185 mμ known to be caused by oxygen-containing anionic impurities. Both phenomena were considerably reduced by treatment of the crystals in chlorine vapor at high temperatures; conversely both were enhanced by growing crystals from melts doped with NaOH, NaOD, and Na₂O₂. There was little evidence, however, that the dopants appeared in these forms in the crystals. Infrared measure-

ments and pH titrations suggested that the most likely result of the dopings was to introduce carbonate into the crystals. The active impurity scattered phonons very strongly at low temperatures; at 5°K approximately 3000 times more strongly than is usually observed for point defects. The cross section was proportional to the first power of the phonon wave vector and was found to be independent of the defect concentration. No detailed model was found to explain these results. A likely explanation would be in terms of an interaction between the phonon field and localized modes of the scattering center.

I. INTRODUCTION

THIS paper describes experimental observations of phonon scattering in certain NaCl crystals that have small amounts of oxygen-containing anionic impurities. The scattering processes were studied by measuring the low-temperature thermal conductivity.

In an insulating crystal, the heat current is carried by phonons and is limited by the scattering processes that these excitations undergo. For a finite, but otherwise perfect, crystal only two types of processes contribute to the thermal resistance: three-phonon umklapp scattering¹ and scattering by the crystal boundary.² The resulting thermal conductivity can be calculated by applying a generalization of a formula derived from kinetic theory³⁻⁷:

$$K = \frac{1}{3} \int C(q) v(q) \Lambda(q) d^3q, \quad (1)$$

where q represents the phonon wave vector (and polarization index), $C(q)$ is the heat capacity per unit volume per normal mode, $v(q)$ is the group velocity of mode q , and $\Lambda(q)$ is the mean free path for this mode. The integration is taken over the first Brillouin zone. At low temperatures the mean free path equals the dimension of the crystal, since umklapp processes are energetically impossible; thus, the conductivity of an ideal crystal increases at T^3 , proportional to the heat capacity. At higher temperatures, the umklapp processes begin to occur, and the mean free path decreases. The conduc-

tivity attains a very high maximum in the vicinity of $1/30$ the Debye temperature and then decreases, first exponentially, then inversely with T as the three-phonon processes become more and more numerous.

This "intrinsic" thermal conductivity is very rarely observed, because real crystals contain defects that make an additional contribution to phonon scattering. First there is isotope scattering, caused by a random distribution of masses.³ Second there are usually other "point" defects present, such as vacancies, interstitials, F centers, and foreign atoms, that scatter because of changes they produce in the interatomic forces. A theory of these effects has been given by Klemens.⁴ His result can be expressed as a cross section:

$$\sigma = (3/\pi) a^2 S^2 (qa)^4, \quad (2)$$

where a^3 is the volume per unit cell. The dimensionless parameter S^2 , which is a measure of the change in atomic mass or in interatomic forces, is of the order of unity for typical point defects. The geometrical cross section is seen to obtain only for large wave numbers ($qa \approx 1$). A detailed comparison between the theoretical prediction based on Eq. (2) and typical experimental results (for example, F centers⁸ in LiF or Ca⁺⁺-vacancy complexes⁹ in KCl) reveals some discrepancies, but agreement within a factor of 2 is usually obtained. The qualitative effect that this type of defect has upon the thermal conductivity is a general decrease on both sides of the conductivity maximum.

Another type of defect is the dislocation, which is predicted to give a low-temperature conductivity proportional to T^2 and hence a lowering of the conductivity curve only on the low-temperature side of the maximum. Experiments were performed by Sproull, Moss, and Weinstock¹⁰ on plastically deformed LiF. Their results confirm the predicted temperature dependence and can be expressed as a scattering "width" W (cross

* Work supported in part by the National Science Foundation and the United States Atomic Energy Commission.

† Present address: Max Planck Institut für Metallforschung, Stuttgart, Germany.

¹ R. E. Peierls, Ann. Physik **3**, 1055 (1929).

² H. B. Casimir, Physica **5**, 495 (1938).

³ P. G. Klemens, Proc. Roy. Soc. (London) **A208**, 108 (1951).

⁴ P. G. Klemens, Proc. Phys. Soc. (London) **A68**, 1113 (1955).

⁵ P. G. Klemens in *Handbuch der Physik*, edited by S. Flügge (Springer-Verlag, Berlin, 1956), Vol. XIV, p. 198.

⁶ P. G. Klemens in *Solid State Physics*, edited by F. Seitz and D. Turnbull (Academic Press, Inc., New York, 1958), Vol. 7, p. 1.

⁷ J. Callaway, Phys. Rev. **113**, 1046 (1959).

⁸ R. O. Pohl, Phys. Rev. **118**, 1499 (1960).

⁹ G. A. Slack, Phys. Rev. **105**, 832 (1957).

¹⁰ R. L. Sproull, M. Moss, and H. Weinstock, J. Appl. Phys. **30**, 334 (1959).

section per unit length of dislocation) given by

$$W \approx 5 \times 10^3 a(qa). \quad (3)$$

This is much larger than the geometrical width, even for long-wavelength phonons.

This paper describes low-temperature thermal conductivity measurements on Harshaw NaCl and certain other NaCl crystals. The results imply a scattering unlike that obtained with ordinary defects; the cross section is of order $a^2(qa)$. The phonon scattering can be correlated with an ultraviolet absorption band at 185 $m\mu$. This band is sometimes referred to as the "hydroxide band"^{11,12}; however, we prefer to call it the "oxygen band," since it is also found in crystals doped with other oxygen-containing anions.¹³

A description will be given of preliminary attempts to identify the nature of the scattering center; the most likely anion is CO_3^{2-} . Finally, a few speculations about the scattering mechanism will be discussed.

II. CRYSTALS

The composition of the thermal conductivity specimens is briefly described in Table I. They ranged in cross section from about 4×4 to about 7×7 mm and in length from 30 to 50 mm. All but one of the crystals received a heat treatment before being mounted for the measurements: They were annealed in an inert atmosphere (usually argon) for at least two hours at 750–760°C. Cooling was controlled and was approximately linear at 1 deg/min to 200°C, at which point the furnace was turned off and allowed to cool by convection to room temperature. This required several more hours.

Crystals were obtained from several sources. Two were commercial synthetic crystals from Harshaw and Optovac. Another was natural rock salt from Baden, Germany.¹⁴ Other crystals were grown at Cornell by the Kyropoulos technique in crucibles machined from National Carbon Company AUC Semiconductor grade graphite. The furnace was vacuum tight, and after it was loaded, it was always pumped to a good fore-vacuum and then filled with a slight over pressure of helium or purified argon.

The Cornell grown crystals received various treatments and dopings. Crystals H' and O' (Table I) were grown from Harshaw and Optovac starting material which had been pretreated in a separate furnace for about 24 hr in one atmosphere of chlorine at 850°C, i.e., 50° above the melting point of NaCl. Crystal V was grown from starting material of Baker and Adamson reagent grade NaCl. For this crystal the crucible was loaded, the furnace sealed, and the load slowly heated

TABLE I. Summary of some of the crystal data. Melt dopings are given in mole fraction. The last two columns give the results of a straight line log-log fit to the low-temperature thermal conductivity data: $K(T) = K_1 T^n$. The units of K are watts/cm-deg. The peak absorption constant for the oxygen band is denoted by $\alpha(185)$.

Crystal number	Host crystal or material	Doping or melt treatment	$\alpha(185)$ (cm ⁻¹)	$K_1 \times 10^4$	n
H	Harshaw	...	7	72	1.82
O	Optovac	...	0.8	1000	1.46
B	Baden	...	0.15		
H'	Harshaw	Cl ₂ -treated	0.32		
O'	Optovac	Cl ₂ -treated	0.18		
V	Reagent	Slowly heated	0.40		
C	Reagent	Cl ₂ -treated	0.26		
1	Heated reagent	4×10^{-4} NaOH	8.3	68	1.87
2	Cl ₂ reagent	10^{-3} NaOH	13.5	52	1.87
3	Heated reagent	10^{-3} NaOH	26	22	2.07
4	Cl ₂ reagent	4×10^{-4} NaOD	8	46	2.09
5	Cl ₂ reagent	3×10^{-3} NaOD	30	8.9	2.32
6	Cl ₂ reagent	6.9×10^{-4} Na ₂ O ₂	67	6.7	2.18

in a vacuum of 10^{-4} to 10^{-5} mm Hg for several days. The procedure outlined by Gardner, Brown, and Janz¹⁵ was followed, in which the heating proceeded in small temperature steps. At each step enough time was allowed for the pressure to drop to its initial low value. In this way most of the adsorbed water could be removed before hydrolysis occurred. Crystal C was grown from material that was heated slowly in an external furnace, under vacuum, and then exposed to slightly less than one atmosphere of chlorine for about 24 hr at 700°C. To reduce subsequent water adsorption by this chlorine-treated salt, it was loaded into the crystal-growing crucible at a temperature of 70–100°C. Then the load was heated overnight at about 400°C while the furnace was evacuated by a fore-pump with a liquid nitrogen cooled trap.

Six crystals were grown from melts doped with NaOH, NaOD, and Na₂O₂. The host material had been previously subjected either to the slow heating or to the chlorine treatment. Dopings are given in Table I. For crystals 2, 5, and 6 they consisted of the appropriate reagent grade material itself. For crystals 1, 3, and 4 the dopings consisted of pieces of a previously grown NaCl crystal, heavily doped to 1–2 mole %. The strength of the latter dopings was determined from pH titration curves performed on aqueous solutions of the doping material.

Spectrochemical analyses were performed on some of the crystals to determine their chemical purity. They are discussed in the Appendix.

III. EXPERIMENTAL PROCEDURE

The technique used in the thermal conductivity measurements has been described in detail elsewhere¹⁶ and

¹¹ J. Rolfe, Phys. Rev. Letters **1**, 56 (1958).

¹² H. W. Etzel and D. A. Patterson, Phys. Rev. **112**, 1112 (1958).

¹³ S. Akpinar, Ann. Physik **37**, 429 (1940).

¹⁴ Catalogue number 62946, Smithsonian Institution, Washington, D. C. The crystal was obtained through the courtesy of Mr. Paul E. Desautels. The thermal conductivity was measured on an unannealed specimen.

¹⁵ H. J. Gardner, C. T. Brown, and G. J. Janz, J. Phys. Chem. **60**, 1458 (1956).

¹⁶ M. V. Klein, Ph.D. thesis, Cornell University, Ithaca, New York, 1961, (unpublished).

was similar to that used in earlier investigations.^{9,17} A steady-state method was used, in which heat was supplied by a heater clamped to the top of the crystal and removed by a heat sink at the bottom. The entire unit was mounted inside a vacuum chamber that was surrounded by a liquid helium bath. The heat sink was connected thermally to the bath by a copper foil. Two "thermodes" were clamped to the crystal to measure the temperature gradient accompanying the flow of heat. The small temperature differences were measured by a combination of carbon resistor thermometers (using an ac Wheatstone bridge¹⁸) and differential thermocouples (using a commercial dc chopper amplifier). The temperatures themselves were deduced either from knowledge of the helium bath vapor pressure or from data taken with a helium gas thermometer, the bulb of which was connected to the heat sink.

Several auxiliary measurements were made to determine the nature and concentration of the phonon-scattering defects. Ultraviolet absorption measurements were performed on a Cary model 14 recording spectrophotometer for photon wavelengths longer than 190 m μ and a vacuum grating spectrometer for shorter wavelengths. Infrared measurements were made on Perkin-Elmer double beam spectrophotometers: the Infracord and the model 21. The presence of atmospheric absorption bands was troublesome; therefore the infrared instruments were flushed with dry nitrogen gas. In addition the sample space was sealed with polyethylene sheeting and exposed to a combination desiccant and CO₂ remover such as NaOH or BaO. Another method used to study the foreign anions in the crystals was that of pH titration. The solid samples were dissolved in freshly boiled water and titrated with dilute acid while the cell was continuously flushed with nitrogen. The use of miniature electrodes made it possible to titrate volumes as small as 1 ml.

IV. EXPERIMENTAL RESULTS

Measurements made early in this work showed that some readily available NaCl crystals have a relatively low thermal conductivity at low temperatures. This can be seen in Fig. 1, where the results of measurements on commercial crystals from Harshaw and Optovac are compared with those on natural Baden halite and two Cornell grown crystals. The Harshaw NaCl results are particularly surprising, especially when they are compared with those for Harshaw KCl,⁹ which show a maximum of 8 w/cm-deg at 6°K, and those for Harshaw LiF,^{8,10} which show a maximum of 20 w/cm-deg at 10°K. The conductivity curves of the Cornell grown crystals, however, are consistent with these KCl and LiF results. In this discussion and in those that follow, the highest conductivity Cornell results (curve C,

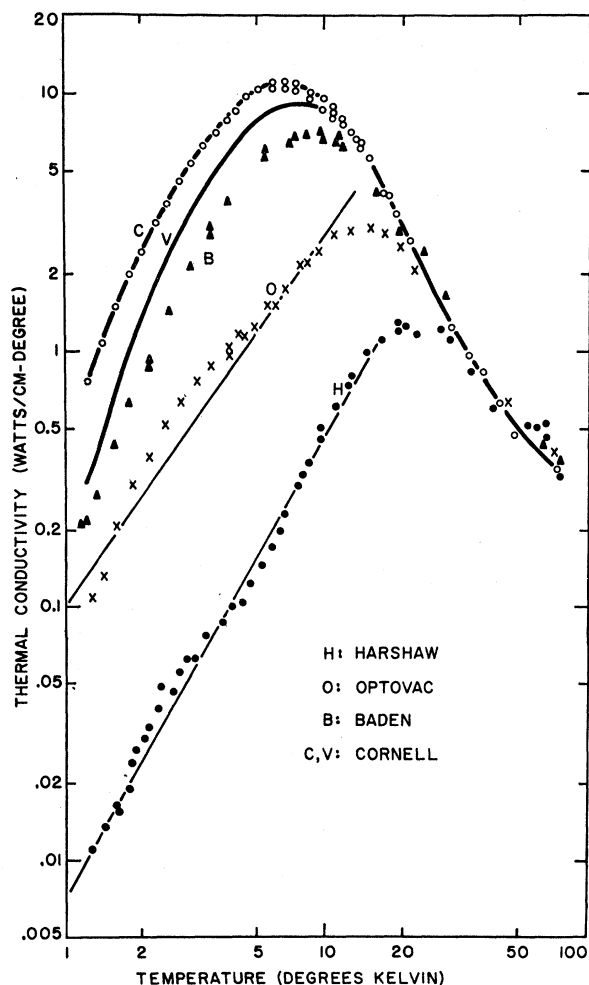


FIG. 1. Thermal conductivity of commercial NaCl crystals from Harshaw and Optovac compared with a natural crystal of Baden halite and two Cornell grown crystals. The straight lines are for a later analysis.

Fig. 1) will be taken as representative of reasonably pure, "well-behaved" NaCl. The anomalous behavior of the commercial crystals can be summarized in the following way: (1) The conductivity is unusually low on the low-temperature side of the maximum only; the high-temperature conductivity values coincide with those for a "pure" crystal. (2) The dependence of K on T is approximately T^2 at low temperatures. (3) The conductivity curves exhibit an unusual inflection in the vicinity of 5°K.

The conductivity of the Baden halite reveals a depression on the low-temperature side of the maximum, but this fact can probably be explained by the presence of physical imperfections in the crystal. Microscopic examination revealed a pronounced mosaic structure, which was also shown by etch pits produced by an alcohol etch (due to Moran¹⁹). In addition the crystal

¹⁷ W. S. Williams, Phys. Rev. **119**, 1021 (1960).

¹⁸ C. Blake, C. E. Chase, and E. Maxwell, Rev. Sci. Instr. **29**, 715 (1958).

¹⁹ P. R. Moran, J. Appl. Phys. **29**, 1768 (1958).

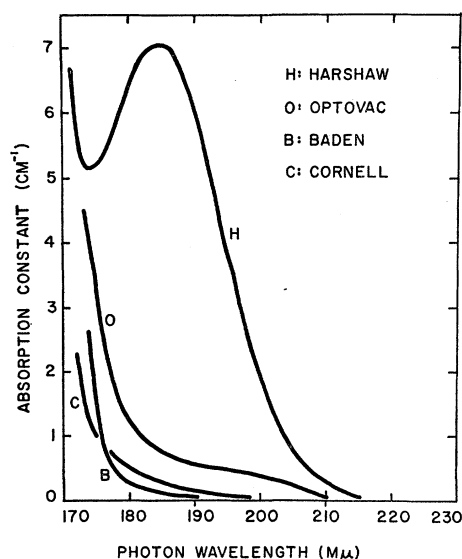


FIG. 2. Ultraviolet optical absorption of four of the crystals described for Fig. 1.

showed a large amount of strain when examined between crossed polaroids. These facts, taken together with the experimental results on the effects of dislocations on thermal conductivity in LiF^{10} strongly suggest that the Baden data can be explained by assuming phonon scattering by dislocations and grain boundaries. It is remarkable that a natural rock salt crystal such as this, which undoubtedly contains many chemical impurities, nevertheless has a conductivity one order of magnitude higher than the usually highly regarded Harshaw material. It appears that the impurities in the halite somehow have become inefficient scatterers of phonons, whereas the commercial crystals contain small amounts of some defect or defects that scatter phonons very effectively at low temperatures.

A clue to the nature of these scatterers is provided by the ultraviolet absorption data shown in Fig. 2. All the crystals show the onset of fundamental absorption at about 175 $m\mu$. Harshaw and to a lesser extent Optovac specimens have an absorption at about 185 $m\mu$, which is the same absorption band found by Rolfe¹¹ and by Etzel and Patterson.¹² They refer to it as the "OH band" because it most likely results from high-temperature hydrolysis of adsorbed water.

Hydroxide is apparently not the only source of this band, however, as has been shown by the work on KCl of Akpınar¹³ and others at Göttingen. Other oxygen-containing anions such as nitrate, nitrite, carbonate, and peroxide produce the same band. For this reason, the band will be referred to here as the "oxygen band."

A comparison of Figs. 1 and 2 shows that a definite correlation exists between the low-temperature thermal resistivity and the size of the oxygen band.

It is known that treatment of crystals at high temperatures in Cl_2 vapor¹³ or HCl vapor¹² can substantially

reduce the oxygen band. With this in mind, crystals were grown from Harshaw and Optovac material that had been exposed in the melt to chlorine for 24 hr. The results are shown in Fig. 3. A significant increase in the conductivity has occurred. The chlorine treatment reduced the 185- $m\mu$ optical absorption also: For Harshaw the absorption constant decreased from 7 to 0.32 cm^{-1} and for Optovac from 0.8 to 0.18 cm^{-1} . The interpretation of these results seems clear: Chlorine treatment removes the source of both the oxygen band and the anomalous low-temperature resistivity.

Corroborating evidence is provided by the results on the two crystals grown from reagent-grade starting material (Fig. 1). Slow heating of the powder in vacuum was not sufficient to produce the highest conductivity values (curve V). An additional high-temperature chlorine treatment was needed (curve C). Chlorine treatment produced the lower oxygen absorption also: The absorption constants at 185 $m\mu$ were 0.26 and 0.40 cm^{-1} for crystals C and V, respectively.

Once it had been established that chlorine treatment could remove the anomalous resistivity and the 185- $m\mu$ absorption band, the next step was to produce both phenomena deliberately by adding appropriate dopings to melts of pure oxygen-free reagent grade NaCl. Results obtained with NaOH dopings are shown in Fig. 4. Hydroxide concentrations in the melts are given in Table I. The conductivity results are quite similar to those for Harshaw, i.e., the high-temperature data show no shift from the values for a pure crystal, and the low-temperature depression has an approximate T^2 de-

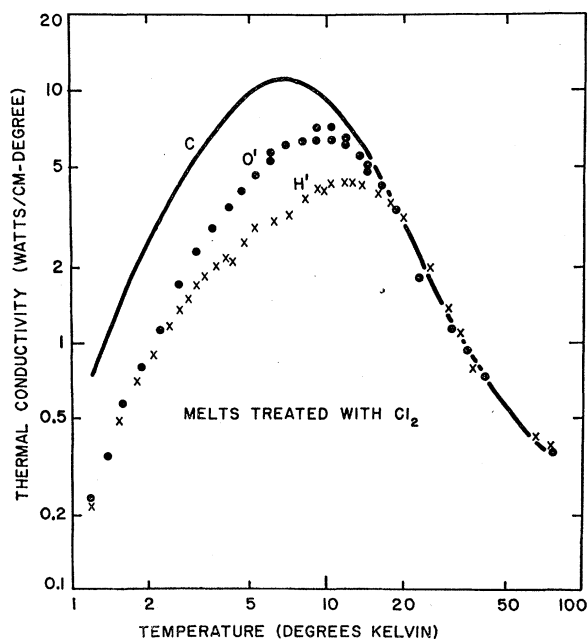


Fig. 3. Thermal conductivity of NaCl crystals pulled from chlorine treated melts starting with Harshaw (H') and Optovac (O') raw material. The best Cornell-grown crystal (C) is shown for comparison.

pendence. The Harshaw curve coincides over all quite well with curve 1. The magnitudes of the oxygen band for crystals 1, 2, and 3 are given in Table I.

Results of melt dopings with NaOD and Na_2O_2 are shown in Fig. 5. The thermal conductivity curves are quite similar to those obtained with NaOH dopings. The sizes of the oxygen band fit in with the general trend.

In order to make a quantitative analysis of the thermal conductivity data, it is necessary to develop a point of view towards the inflection at 5°K, which is present in some of the curves to a much greater extent than in others. For the time being, the attitude taken here will be that the inflection is a manifestation of a secondary, minor impurity state, whose absence or presence does not detract from the primary effect, namely the approximate T^2 depression of the conductivity on the low-temperature side of the maximum. This was the motivation for drawing the straight lines in Figs. 1, 4, and 5. Their position and slope will be taken as suggestive of the primary effect of the impurities. The parameters that characterize these lines are given in Table I along with the sizes of the oxygen

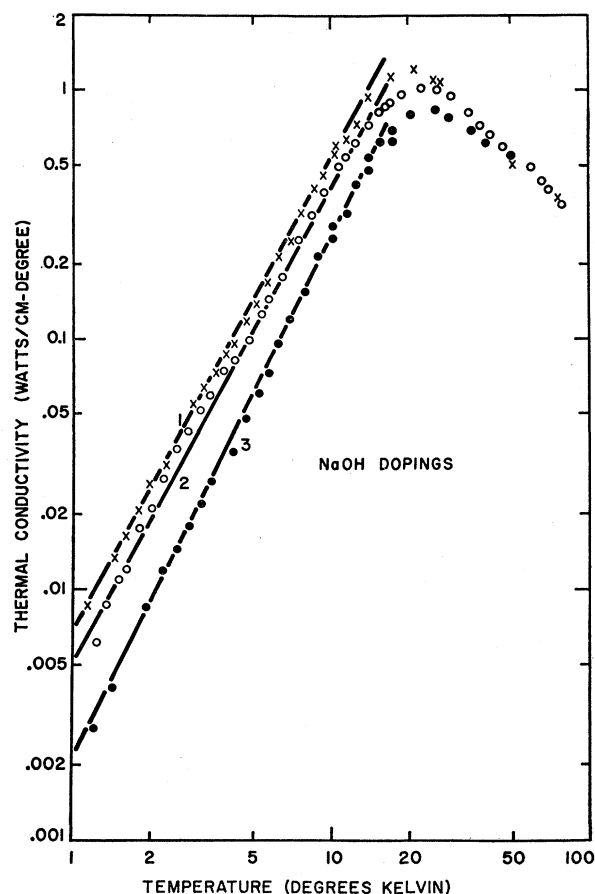


FIG. 4. Thermal conductivity of NaCl crystals pulled from melts to which NaOH had been added. The dopings are given in Table I. The straight lines are for a later analysis.

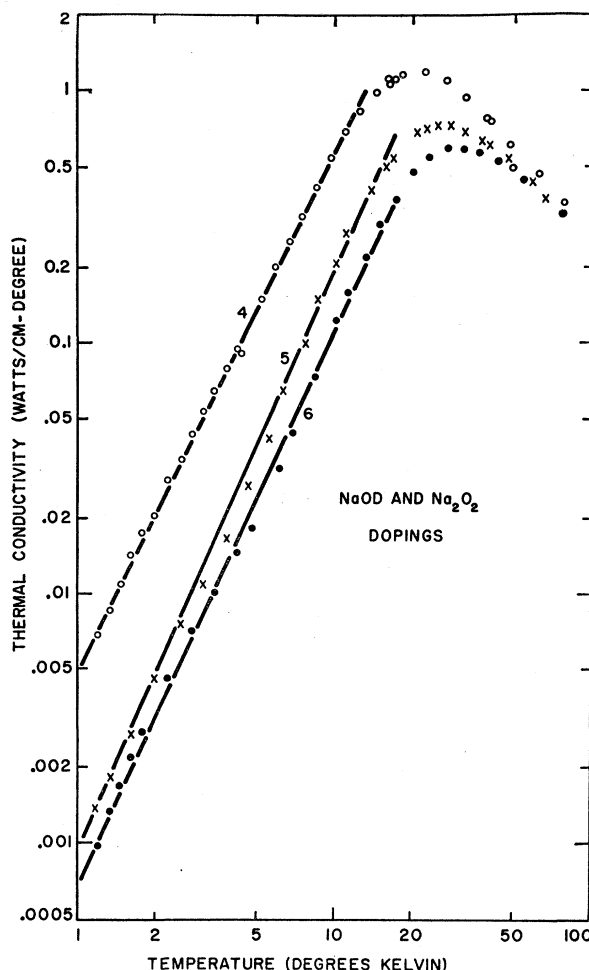


FIG. 5. Thermal conductivity of NaCl crystals grown from melts doped with NaOD (curves 4 and 5) and Na_2O_2 (curve 6). The dopings are given in Table I.

band. Data on the extrapolated resistivities at 1° and 10°K are plotted against the absorption constant in Fig. 6. A definite correlation is seen to exist.

V. ATTEMPTS TO IDENTIFY THE ACTIVE SCATTERERS

The identification of the defect responsible for the observed low-temperature resistivity has not been made with assurance. In general, it cannot be assumed that the chemicals that appear in the finished crystal were those that were added to the melt. For example, even a short exposure of NaOH pellets to the air results in their being covered with a layer of Na_2CO_3 . Thus, all hydroxide and deuterioxide doped melts contained some carbonate as well. The effective distribution coefficient of Na_2CO_3 in NaCl is not known. If it were much higher than that of NaOH, the crystal might contain more carbonate than hydroxide, even though the opposite might be true in the melt.

Additional carbonate in these melts could possibly

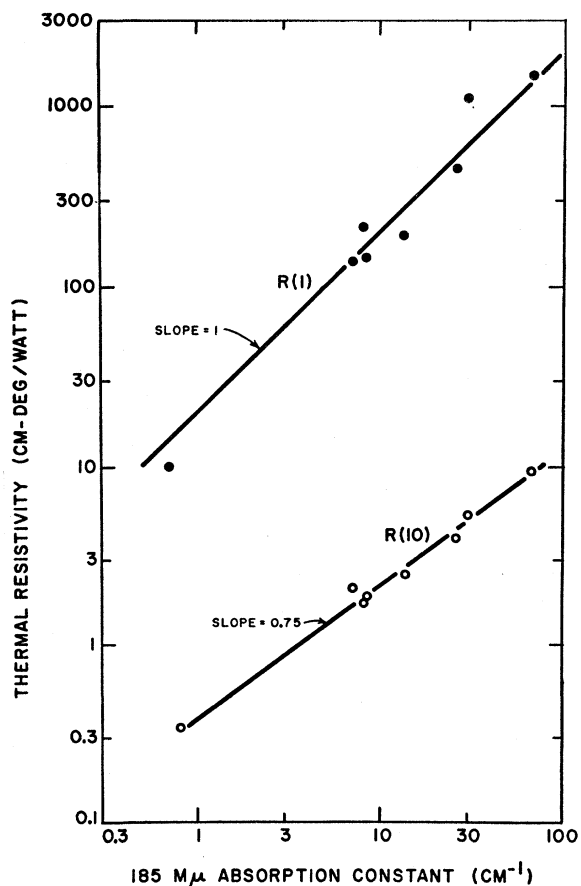


Fig. 6. Comparison of thermal resistivity at 1° and 10°K with the strength of the 185-m μ oxygen absorption band.

result from a high-temperature reaction of hydroxide with the graphite crucible. The extent to which this reaction occurred is not known. It could have been avoided by growing the crystals from silica crucibles; however, this would have introduced silicate contaminants, and it was originally felt that these would have been even more undesirable than carbonate. With the peroxide doping there was undoubtedly carbonate present also, for pure Na_2O_2 is known to react strongly with powdered charcoal at high temperatures to form Na_2CO_3 and Na metal.²⁰

The titration method was used to determine the alkalinity of the pieces of the heavily doped boules that were the sources of hydroxide and deuterioxide for crystals 1, 3, and 4. At these concentrations of 1–2% there was no trouble getting good results. Three inflections in the titration curves were noticeable. They were taken as evidence that the initial crystals contained OH^- and CO_3^{2-} in a proportion of about 6:1; the end points were interpreted as neutralization points for OH^- , CO_3^{2-} , and HCO_3^- , respectively. This interpretation was supported by agreement between the measurements and

a theoretical calculation of the pH values at each end point.

The picture that resulted from titration of samples from the final boules was different. The combination of very strong electrolyte plus very dilute base often gave erratic data. When the data were reproducible, they showed two approximately equally spaced end points. These were interpreted as the carbonate and bicarbonate end points. There was no inflection that could correspond to a hydroxide end point. A small quantity of hydroxide could have been present with an unresolved end point, since the amount of acid added at the first end point was slightly more than half the total at the second. This difference would correspond to the presence of about 10% hydroxide and 90% carbonate, but the data were not good enough to make this a solid conclusion.

These results support the hypothesis stated above: In spite of a larger amount of hydroxide in the melt, the crystals contain mostly carbonate. Another piece of evidence is furnished by the appearance of the boules. The bottom ends of some of them were cloudy and gave the appearance of the segregation of a second phase. This would be difficult to understand if only hydroxide were present in the crystal, for the room temperature solubility of NaOH in NaCl is supposed to be several percent.²¹ On the other hand, if carbonate were the main impurity, it might cause the precipitation; this would indicate that it is very insoluble in NaCl. Some of the samples titrated came from such cloudy regions. A typical end point corresponded to a carbonate concentration of 7×10^{-5} mole fraction. This, then, would be an upper limit of the effective solubility of carbonate in NaCl. Results of titrations on other cloudy samples agreed with this figure within a factor of 2. No independent information about the solubility of Na_2CO_3 in NaCl could be found.

The infrared results were not very satisfactory. This can be attributed partly to small sample size; these measurements were made after the boules had been cleaved for all the other measurements. The O-H vibrational absorption band at 2.8μ was scarcely observable. When it was seen, its area was only 10% the areas of two other more prominent bands which occurred at 6.45 and 7.10μ . The integrated areas of these two strong bands were about equal. A strong $7.10\text{-}\mu$ absorption was always accompanied by a weaker $11.35\text{-}\mu$ absorption. The 7.10 and $11.35\text{-}\mu$ bands can be attributed to carbonate, as they have been found in Na_2CO_3 mulls by Miller and Wilkins,²² in NaCl: Na_2CO_3 pellets by the author, and KCl: K_2CO_3 and KBr: K_2CO_3 mixed crystals by Maslakowez.²³

The other strong band, that at 6.45μ , has not been identified. It was not found in the NaCl: Na_2CO_3 pellets, nor could it be identified in any of the spectra of

²¹ Reference 20, p. 369.

²² F. A. Miller and C. H. Wilkins, *Anal. Chem.* **24**, 1253 (1952).

²³ F. Maslakowez, *Z. Physik* **51**, 696 (1928).

²⁰ *Gmelins Handbuch der Anorganische Chemie* (Verlag Chemie GMBH, Berlin, 1928), No. 21, p. 242.

the 159 inorganic ions given by Miller and Wilkins.²² Perhaps it is related to the double band they found at 6.02 and 6.15 μ in NaHCO₃; however it is difficult to know whether any bicarbonate survived the high melt temperature. Wardzyński found a band at 6.56 μ in KCl:KOH,²⁴ but few details were given, and it is difficult to decide what his crystal really contained.

As mentioned above, the 2.8- μ O-H band was very weak, if present at all. The corresponding 3.6- μ O-D band was not found, even in the strongly (1%) deuterioxide doped boule. This boule, however did give a titration curve consistent with the assumption that the principal basic impurity was OD⁻ (or OH⁻). The reason for this discrepancy is not known. The heavily OH-doped boule was cloudy and polycrystalline and was therefore not suitable for infrared measurements.

The strengths of the 2.8- and 7.1- μ bands were calibrated against those measured on pellets pressed from mixtures of carbonate and hydroxide with NaCl. The pressure used was limited by the press to 56 ton/in.²; better cakes would have resulted at higher pressures. Under these conditions, the pellets were not very transparent; however, a rough estimate of the concentration did result. The conversion factors were 2.5×10^{18} NaOH molecules per cm³ for 1 cm⁻¹- μ and 2.0×10^{18} Na₂CO₃ molecules per cm³ for 1 cm⁻¹- μ . These results are in rough agreement with the value 1.16×10^{18} /cm²- μ calculated from classical dispersion theory for a proton oscillator. Smakula's equation²⁵ was used, but corrected for the mass of the proton. The local field correction used was that for electrons.

Comparisons among the results of the three types of measurements (ultraviolet absorption, infrared absorption, and pH determinations) were made to check consistency. The total concentration of infrared-active centers (bands at 2.8, 6.45, 7.10, and 11.35 μ) was determined using the experimental conversion factors mentioned above. The strength value for the 6.45- μ band was taken to be the same as that for the 7.10- μ band. These totals were compared with concentration values computed from the 185-m μ ultraviolet absorption data using Etzel's conversion factor of $(2.8 \times 10^{15} \text{ absorbers/cm}^2 \pm 50\%)$ per unit absorbance.²⁶ The infrared determined values were consistently lower by an average factor of about 3. No infrared absorptions at all could be observed for a Harshaw crystal. The sensitivity was such that the upper limit of the ratio of infrared to ultraviolet determined concentration values was 0.4.

Concentrations of alkaline impurities were determined from the titration curves, when these seemed reliable, and were compared with the ultraviolet absorption results. The comparison could be expressed as an oscillator strength²⁵ for the absorption, which came

out to be about 0.2. This is 10% of the oscillator strength that one calculates from Etzel's conversion factor. The value 0.2 also disagrees with the value of about 0.8 that was found by Mollwo and Pohl for the analogous 205-m μ band in carbonate doped KCl.²⁷

Thus the identification of carbonate as the major anionic impurity still is uncertain; there are many contradictions that must be resolved, for instance, the completely negative infrared results with the Harshaw crystal. Perhaps Harshaw crystals contain neither hydroxide nor carbonate, but oxygen in a noninfrared absorbing form, say O₂⁻.²⁸ The present evidence does indicate, however, that the anions in the Cornell grown crystals are more likely to be carbonate than hydroxide.

VI. INTERPRETATION OF RESULTS

The experimental results can be summarized by saying that the low temperature conductivity was approximately T^2 with a coefficient (at 1°K) inversely proportional to the strength of the oxygen band and with an exponent that tended to increase slowly with increasing optical absorption. (See Table I.) This discussion will ignore any deviations of the exponent from 2.

For a quantitative discussion of the results, it is useful to consider the data for a representative crystal. We will take crystal 1, having the results shown in Fig 3 and Table I. It follows from the form of Eq. (1) that if Λ^{-1} varies as q^n , then at low temperatures K must vary as T^{3-n} . The observed temperature dependence then implies that $n=1$. It was possible to integrate Eq. (1) numerically using a simple addition of reciprocal mean free paths determined from theoretical expressions for isotope scattering and three-phonon scattering. (The method was that given by Callaway⁷ and applied by Pohl.⁸) An excellent fit to the data for crystal 1 was obtained with a dominant low-temperature reciprocal mean free path equal to $3.3 \times 10^{-5} q \text{ cm}^{-1}$.

To calculate a scattering cross section from the mean free path data, the defect concentration is needed. As already mentioned, this has not been uniquely determined. A concentration estimate can be made from the ultraviolet absorption results by the use of Smakula's equation²⁵:

$$nf = 1.3 \times 10^{17} \frac{n'}{(n'^2 + 2)^2} \alpha_m W. \quad (4)$$

Here n is the number of absorbers per cm³, f the "oscillator strength," n' the index of refraction, α_m the peak absorption constant in cm⁻¹, and W the width of the absorption band at half-maximum in electron volts. For the 185-m μ band one can take²⁹ $n'=1.89$ and

²⁷ E. Mollwo and R. W. Pohl, *Ann. Physik*, **39**, 22 (1941).

²⁸ W. Känzig and M. H. Cohen, *Phys. Rev. Letters* **3**, 509 (1959).

²⁹ F. Martens, *Ann. Physik* **6**, 603 (1901), as quoted by *American Institute of Physics Handbook* (McGraw-Hill Book Company, New York, 1957), pp. 6-23.

²⁴ W. Wardzyński, *Acta Phys. Polon.* **17**, 29 (1958).

²⁵ F. Seitz, *Modern Theory of Solids* (McGraw-Hill Book Company, Inc., New York, 1940), pp. 662-664.

²⁶ H. W. Etzel (private communication). See also Reference 12.

$W = 24.4 \text{ m}\mu$ or 0.884 eV . The result is $nf = 0.71 \times 10^{16} \alpha_m$. For the crystal under consideration, we have $\alpha_m = 8.3 \text{ cm}^{-1}$, so that the right side of Eq. (4) becomes $5.9 \times 10^{16} / \text{cm}^3$. Etzel's estimate of f was about 2.5 .¹² This would give a density of absorbers of $2.4 \times 10^{16} / \text{cm}^3$, which corresponds to 10^{-6} mole fraction. The titration results for this crystal put the impurity concentration at about 10^{-5} mole fraction; thus we are left with a factor of 10 uncertainty. For the remainder of this discussion the higher concentration value (10^{-5} mole fraction) will be used.

With $\Lambda^{-1} = 3.3 \times 10^{-5} q$ and $n = 2 \times 10^{17} / \text{cm}^3$, the scattering cross section can be computed:

$$\sigma = (\Lambda n)^{-1} = 3.3 \times 10^{-5} q n^{-1} = 1.65 \times 10^{-22} q.$$

Introducing the molecular volume, $a^{-3} = 2.23 \times 10^{22} \text{ cm}^{-3}$, we can write

$$\sigma = 3.7 a^2 (qa). \quad (5)$$

This should be compared with the cross section for an ordinary point defect, Eq. (2). The ratio is

$$\sigma / \sigma_{pt} = 4 (qa)^{-3} S^{-2} \cong (qa)^{-3} \approx [\hbar v / (akT)]^3, \quad (6)$$

where a dominant phonon argument has been used to convert from q to T . At 5°K this ratio is about 3000.

The implications of the experimental results and the burden they place upon their interpretation are now apparent. Any scattering model must produce a cross section per impurity that is several orders of magnitude greater than that for Rayleigh scattering. This is not easy to do, and as yet no model has been found that meets the requirements. Two general types have been suggested; these will now be discussed, and the difficulties that arise from their application will be mentioned.

Models that Rely on Coherent Scattering

These models begin with the assumption that the scattering cross section for an isolated defect is a reasonably well behaved quantity, for example a Rayleigh scattering cross section with an S^2 of order unity [Eq. (2)]. The basic idea of this approach is that the measured cross section is much larger than this because of the coherent addition of scattered amplitudes from neighboring defects. This enhancement can be accounted for in the theory by multiplying the single particle probability for phonon scattering from \mathbf{q} to \mathbf{q}' by the factor $|f(\mathbf{q}' - \mathbf{q})|^2$, where $f(\mathbf{q}' - \mathbf{q})$ is the $\mathbf{q}' - \mathbf{q}$ Fourier component of the distribution function $f(\mathbf{r})$ that gives the concentration of impurities at \mathbf{r} .³⁰ If it is assumed that the single particle cross section is of the Rayleigh type, then the data force $|f(q)|^2$ to be proportional to q^{-3} . The corresponding spatial dependence of $f(r)$ would vary with the assumed symmetry of the probability distribution.

With spherical symmetry it is easy to show that f

must be proportional to r^{-3} . It is difficult to imagine any mechanism that could produce this distribution, but even if one could exist, a dimensional argument will show that the resulting cross section is too small. The reasoning goes as follows: Let the point defects have average density n and be distributed about N randomly located spheres per unit volume. The average radius of the spheres will be denoted by R . Then $f(r)$ will be approximately $(n/2)R^3 r^{-3}$. (This averages to n in the volume of one sphere.) After performing the Fourier transform, we get $f(q) = \sqrt{2} \pi^{3/2} n R^3 q^{-3}$ for each sphere. Then for the entire crystal of volume Ω , we get $|f(q)|^2 = 2 \pi^3 N n^2 R^3 q^{-3}$. In calculating σ , a factor Ωn is removed. In addition we can set $\frac{4}{3} \pi R^3 N = 1$. The resulting ratio of cross sections is

$$\sigma / \sigma_{pt} \approx 15 \rho (qa)^{-3}, \quad (7)$$

where ρ is the average defect concentration expressed in mole fraction. This result is several orders of magnitude less than the experimental result, Eq. (6). In addition, it predicts a concentration-dependent cross section, in direct contradiction to the experimental facts (Fig. 6). The inclusion of angular dependence in $f(r)$ will not alter the order of magnitude of the computed cross section.

With the assumption of cylindrical symmetry, one can write

$$|f(q)|^2 = |f(q_1)^{(2)}|^2 / (q_z \Omega^3),$$

where q_1 and q_z are the components of q normal and parallel to the symmetry axis and $f^{(2)}$ is the two dimensional distribution function in the normal plane. Now the requirement becomes $|f^{(2)}|^2 \propto q^{-2}$, which can be satisfied by an $f^{(2)}(r) \propto l/r$, with l a parameter. Such a distribution might occur around dislocation lines. A normalization argument similar to that applied in the spherical case requires l to be about equal to the average distance between dislocations.

The exact calculation of $f^{(2)}(q)$ will not be given here, but the order of magnitude result is given by Eq. (7) with a slightly different numerical factor. The conclusion seems to be that no coherent scattering mechanism is able to explain the experimental facts.

Models Based on an Anomously Large Point-Defect Scattering Cross Section

Consideration of the types of interaction that could lead to the observed cross sections suggests almost immediately a resonance scattering. In fact every scattering mechanism that does not involve changes in internal degrees of freedom of the scatterer seems to lead, for long wavelengths at least, to the familiar Rayleigh scattering cross section.

Whereas resonance scattering can produce a very large cross section for selected values of the phonon wave vector, it has not been possible so far to derive from this any well-behaved temperature dependence for the thermal resistivity. The difficulties become evi-

³⁰ P. Carruthers, Revs. Modern Phys. **33**, 92 (1961).

dent upon consideration of scattering by the simplest system having internal degrees of freedom, a "two-level atom." The interaction between a given phonon and this atom will depend upon whether or not the interactions between the atom and other phonons can be neglected. If they can, the phonon under consideration will interact by virtual absorption and re-emission (resonance fluorescence). The cross section will have a strong, almost singular, energy dependence for energies near the atomic level spacing, ΔE . The general case of many phonon interactions with the atom is complicated, but it simplifies in the limit of strong interaction. In this case, coherent re-emission is prevented; the given phonon is physically absorbed; and re-emission of an uncorrelated phonon occurs. In this case, a strong "resonant" cross section also obtains.

In both cases, a noticeable decrease in the mean free path occurs only for a small set of q values. If the thermal conductivity is computed by Eq. (1), the result will be to decrease or even omit those terms in the integral that have these q values. Since there are only a few such terms, the effect on the integral will be small.

This result is probably wrong. If there is strong resonance for only a few modes, the normal (non-umklapp) three-phonon scattering processes will spread the effect over all neighboring modes. The correct calculational procedure might be quite complicated, but an estimate can be obtained from the "harmonic mean" formula, which is the correct solution of the Boltzmann equation in the limit of very strong normal processes.^{31,32} This formula says that the conductivity should be calculated from

$$\frac{1}{K} = \frac{3}{C^2} \int \frac{C(q)}{v(q)\Lambda(q)} d^3q.$$

Because σ and hence $1/\Lambda(q)$ behaves much like a delta function, the value of the integral is approximately the integrand evaluated at resonance where $q = \Delta E/(\hbar v)$. Because of the temperature dependence of $C(q)$ and $\Lambda(q)$, the resulting expression for K^{-1} will have a complicated product of exponential and power-law temperature dependence, which will not approximate T^{-2} over the required temperature range.

Phonon scattering by a many-level system would produce a sum of such terms for K^{-1} , but at the moment it seems that there would be enough "graininess" in the result to keep it from having the required temperature dependence. A more sophisticated theoretical treatment of this problem (including a better solution of the Boltzmann equation having a singular or nearly singular kernel) might avoid this difficulty.

Another explanation for these experimental results might be a relaxation process. The orientation of the active center would be assumed to be sensitive to de-

formation, but the center would not be able to keep in phase with a rapidly varying stress (phonon). Such a mechanism would then give rise to dissipation and scattering. This mechanism has an important element in common with a resonance mechanism, namely, it involves local degrees of freedom that can be activated at low temperatures and that couple strongly to the phonon field. It seems that the correct explanation of the strong low-temperature phonon scattering must involve such internal modes.

It is tempting to attribute the inflection observed near 5°K in some of the crystals, particularly Harshaw, to a resonance interaction. It might then be difficult to explain why the strength of the inflection varied so much from crystal to crystal. One explanation is that this observation was a manifestation of small changes in the energy level structure of the scatterers, perhaps because of interactions with other impurities.

Until the nature of the scattering center is known more exactly, it does not seem appropriate to carry these speculations any further. An interesting possibility for the future is that this center and its energy levels will be revealed by other experimental techniques, for example, detailed infrared measurements perhaps carried out at helium temperatures.

VII. CONCLUSION

A strong phonon scattering process has been found in NaCl that is directly related to the presence of some oxygen-containing ion or ions. The identification of the scatterer as carbonate was only tentatively made; confirmation awaits the results of thorough analyses of crystals grown using more careful doping procedures. Until a reliable identification is made, only speculations exist about the details of the interaction between the impurity and the phonons. At the present time, a resonance-type mechanism appears to be the most attractive.

ACKNOWLEDGMENTS

The author wishes to thank Professor R. L. Sproull for his guidance throughout this investigation. He also wishes to thank Professor R. O. Pohl for many discussions and suggestions, Professor R. Brout, Dr. P. Caruthers, and Dr. G. Peterson for discussions about the theory, Dr. H. Mahr and Mr. T. Timusk for performing vacuum ultraviolet measurements, Professor D. Cooke for help with some of the chemistry, and Mr. J. Ashe for growing the crystals.

Finally, the author wishes to thank the National Science Foundation for fellowship support during the early stages of this work.

APPENDIX. SPECTROCHEMICAL ANALYSIS

Semiquantitative spectrographic analyses for traces of metallic impurities were performed by W. B. Coleman & Company, Philadelphia, Pennsylvania. They also did a quantitative analysis for calcium. Results (in parts

³¹ J. M. Ziman, *Electrons and Phonons* (Oxford University Press, New York, 1960), p. 308.

³² J. M. Ziman, *Can. J. Phys.* **34**, 1256 (1956).

per million by weight) for Harshaw were: Ca, 270; Fe, 100-1000; Al, 10-50; Cu, 10-100; Si, 5-10. Results for crystal *C* ("purest" Cornell grown crystal) were Ca, 400; Fe, <10; Al, 10-100; Cu, <2; Si, <50. The results of the calcium determinations were suspected to be incorrect, and they were repeated in an apparatus

especially designed to detect small amounts of Ca in the presence of alkali halides.³³ The results were 47 ppm for Harshaw and 50 ppm for crystal *C*. These lower figures are believed to be much more reliable.

³³ The measurements were performed by Q. Won Choi of the Cornell University Chemistry Department.

Magnetic Structure of Chromium Selenide*

L. M. CORLISS, N. ELLIOTT, J. M. HASTINGS, AND R. L. SASS†

Department of Chemistry, Brookhaven National Laboratory, Upton, New York

(Received January 31, 1961)

The magnetic structure of the NiAs-type compound, CrSe, has been determined by means of neutron diffraction. The indexing of superstructure lines which appear below the Néel point requires a unit cell three times as large as the conventional unit ($a = \sqrt{3}a_{\text{NiAs}}$). Planes parallel to the basal plane contain three chromium atoms whose spins form an "umbrella"-like array with threefold symmetry. Individual moments alternate in sign along lines parallel to the *c* axis. A value of $2.90 \mu_B$ has been deduced for the component of the chromium moment perpendicular to the *c* axis.

INTRODUCTION

A LARGE number of the sulfides, selenides, and tellurides as well as arsenides and antimonides of the transition metals have the nickel arsenide crystal structure. This structure, shown in Fig. 1, consists of a hexagonal close packing of the metalloid atoms with the transition metal atoms located in the interstices in such a way as to form a simple hexagonal array. The bond character as well as magnetic properties of these compounds and their solid solutions cover a rather wide spectrum. Some of the sulfides, such as CrS, are thought to be ionic, while the arsenides and antimonides, such as MnAs, are most probably covalent or metallic. Because of this range in bond character, the nature of the magnetic interaction can be expected to vary all the way from a direct (metallic-bond type) to an indirect (ionic bond) exchange mechanism. Some of the compounds,

e.g., CrS and MnTe, are antiferromagnetic while others, e.g., CrTe and MnAs, are ferromagnetic. The magnetic properties of these materials as well as solid solutions have been extensively investigated in recent years. In particular, the system¹ $\text{CrSe}_{1-x}\text{Te}_x$ has been examined and the pure compound CrSe was shown to have an anomalous temperature dependence of its susceptibility. The magnetic susceptibility data of Tsubokawa and of Lotgering and Gorter are shown in Fig. 2. The anomalies present in both sets of data below 300°K have led these authors to suggest a transition to an antiferromagnetic state. More recent measurements by Tsubokawa,² performed on single crystals of CrSe, indicate a Néel point close to 300°K and an effective moment of $4.90 \mu_B$, corresponding to a spin of 2 if the orbital moment is completely quenched. The paramagnetic moment reported by Lotgering and Gorter is approximately 10% lower than that given by Tsubokawa. A neutron

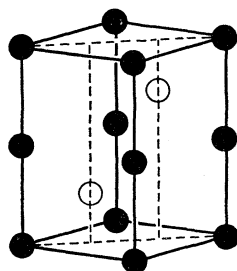


FIG. 1. Structure of CrSe.

● CHROMIUM
○ SELENIUM

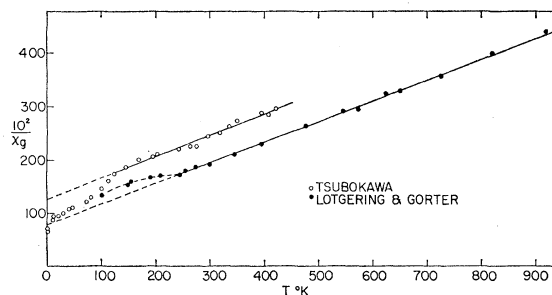


FIG. 2. Reciprocal susceptibility of CrSe as a function of temperature.

* Research performed under the auspices of the U. S. Atomic Energy Commission.

† Permanent address: The Rice Institute, Houston, Texas.

¹ I. Tsubokawa, J. Phys. Soc. Japan **11**, 662 (1956); F. K. Lotgering and E. W. Gorter, J. Phys. Chem. Solids **3**, 238 (1957).

² K. Adachi (private communication).